Phase analysis of interferometric DoA estimation in linear phased array radars

Vitor Augusto F. Santa Rita[1] e Mateus Dantas Lins de Oliveira[2]
[1]Brazilian Army Technological Center, Rio de Janeiro/RJ - Brazil
[2]Brazilian Army Technological Center, Rio de Janeiro/RJ - Brazil

***Abstract*— It is analyzed the phase difference of two sub-arrays as a function of DoA upon tapering in a uniform linear antenna array. The function is linear when a constant taper is used and, in the design of an antenna, it is interesting to keep the phase relation linear and also to have a symmetrical taper to suppress side lobes levels, but it is proven that it is not possible; any symmetrical non-constant taper used to suppress side lobe levels distorts the linear phase relation. There is a trade-off between the linear phase relation and low side lobes levels. To handle the phase distortion, a mathematical expression for the phase curve is obtained, and an ML algorithm is designed with it. This algorithm has same performance results in mean square error compared to a look-up table with linear interpolation of the phase monopulse ratio. It is also shown how to obtain a analytical characterization of the Cramer-Rao lower from the mathematical expression, and this result is used to show that the ML algorithm and the linear interpolation of the phase monopulse ratio are both optimal, achieving the Cramer-Rao bound.**

***Palavras-Chave*— direction of arrival, radar interferometry, maximum likelihood estimation.**

I. Introduction

Uniform linear array (ULA) antennas are an important technology for the research and development in the radar field that allows the antenna radiation pattern to be shifted and modified in a direction of interest. A taper is commonly used in the transmission and reception of signals to suppress side lobe levels, but it distorts the received signal phase as a undesired consequence. In this article, it is investigated a particular 3D phased array antenna in which the vertical elements are built in a static setup, with taper to widen vertical covered combined with a upper digital rotation to avoid power transmitted to ground.

In this research, the theoretical results describing the phase difference based on the Direction of Arrival (DoA) are used to develop a Maximum Likelihood (ML) estimator. The ML estimation is a well known approach to obtain an value $\hat{a}(R)$ from observations R of an experiment as the estimate of an unknown parameter A at which the likelihood function $p(R|A)$ is a maximum [1]. This means in summary that $\hat{a}(R)$ is the most likable correct value of A.

When the subarrays are tapered for sidelobe control, the locations of phase centers are shifted as a function of DoA angle [2], so it requires additional digital processing for interferometric DoA estimation. However, spectral-based techniques with decomposition of the covariance matrix as MUSIC, Root-MUSIC and ESPRIT require the output of all elements be available [3] so are not adequate to subarrays. Thus, it is chosen the ML and monopulse estimators for the analysis, the latter designed specifically to subarrays.

Interferometry from taper in subarrays is handled in [4] with an Extended Phase Interferometry estimator that includes both phase and amplitude. The performance comparison of DoA estimators in subarrays with taper is seen in [5], comparing ML and modified interferometry and monopulse algorithms through look-up table interpolation and polynomial approximation. The best performance is of the look-up table with linear interpolation of the phase monopulse ratio.

This paper clarifies the underlying mathematical bases of the *phase curve* distortion as a function of a taper. And allows further the development of a ML estimation and the deduction of the Cramer-Rao bound for the problem of interferometry estimation.

The paper results offer an approach to surpass the problem of phase distortion, allowing the design of an antenna array in the research and development of a radar to consider both the side lobe levels and phase distortion problems combined.

A better azimuth or elevation estimation provides a more precise identification of targets at longer distances. It also allows a cost reduction in the hardware of a radar as compensation due to the more capacity localized in the algorithms.

The paper is organized as follows. In section II, the antenna model is described. In section III, it is analyzed the relation of the *phase curve* of a taper for digital rotation. In section IV, it is investigated if there exist a type of symmetrical non-constant windowing that keep the *phase curve* unaltered, which would guide the analysis to it, but it is shown it does not exist. In section V, a mathematical expression of the *phase curve* is obtained. In section VI, a simple ML DoA estimator is developed, exploring the mathematical expression, giving also its Cramer-Rao lower bound. Performance evaluation is in section VII. Finally, section VIII concludes.

II. ULA Antenna Model

The ULA contains two subarrays each with m-elements, totaling $N_a = 2m$ elements. The model is in the horizontal position in Fig. 1. The inter-element distance is d.

The DoA is represented by θ, and in ψ-space it is given by $\psi = 2\pi \frac{d}{\lambda} \sin(\theta)$, with $\theta \in [-\pi/2, \pi/2]$ so that $\psi \in [-\pi, \pi]$. The angle ψ is used from now on to mean angle of arrival in ψ-space.

The vector of received signals in base band at an instant t is $\boldsymbol{x}(t)$:

$$\boldsymbol{x}(t) = \alpha p(t) \boldsymbol{a}(\psi) + \boldsymbol{n}, \tag{1}$$

V. A. F. Santa Rita, vitoraugusto.rita@eb.mil.br; M. D. L. de Oliveira, mateus.dantas@eb.mil.br.

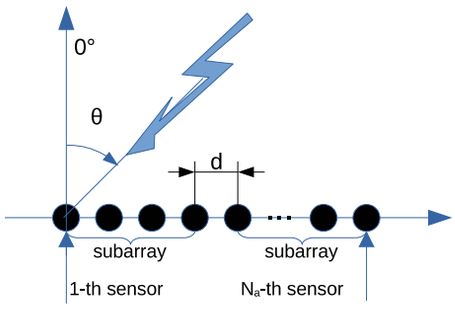

Fig. 1. ULA with N_a omnidirectional elements.

in which α is the amplitude, $p(t-\tau)$ is the received pulse, $\boldsymbol{a}(\psi)$ is the array manifold vector of target azimuth ψ and $\boldsymbol{n}$ is the noise: a random variable with null mean, white color (signal whose spectrum has equal power within any equal interval of frequencies), circular, complex and with gaussian distribution.

Beamformings in subarray are done with $\boldsymbol{w}_1$ and $\boldsymbol{w}_2$ as follows:

$$\boldsymbol{w}_1 = [\boldsymbol{w}_1^0 \quad \dots \quad \boldsymbol{w}_1^{m-1} \quad 0 \quad \dots \quad 0]^T, \tag{2}$$

$$\boldsymbol{w}_2 = [0 \quad \dots \quad 0 \quad \boldsymbol{w}_2^m \quad \dots \quad \boldsymbol{w}_2^{2m-1}]^T. \tag{3}$$

Then, the matrix $\boldsymbol{W} = \begin{bmatrix} \boldsymbol{w}_1 & \boldsymbol{w}_2 \end{bmatrix}$ is a $N_a \times 2$ matrix with all elements real values, being $w_1^k \geq 0$ and $w_2^k \geq 0$ the k-th element in the vector.

The observation vector $\boldsymbol{r}$ from beamformings at an instant t is

$$\boldsymbol{r} = \boldsymbol{W}^H \boldsymbol{x}(t) = \begin{bmatrix} r_1 \\ r_2 \end{bmatrix}. \tag{4}$$

III. Phase curve upon beam taper for rotation

Consider $\boldsymbol{W}$ includes tapering for rotation ψ_r as

$$\boldsymbol{W} = [\boldsymbol{w}_1 \circ \boldsymbol{a}(\psi_r) \qquad \boldsymbol{w}_2 \circ \boldsymbol{a}(\psi_r)], \tag{5}$$

in which $(.) \circ (.)$ is the Hadamard product operator.

Admitting $\alpha p(t) = 1$ and noise-free in (1) for simplicity, $\boldsymbol{r} = \boldsymbol{W}^H \boldsymbol{x}(t)$ in an instant t is

$$\boldsymbol{r} = \begin{bmatrix} (\boldsymbol{w}_1 \circ \boldsymbol{a}(\psi_r))^H \boldsymbol{a}(\psi) \\ (\boldsymbol{w}_2 \circ \boldsymbol{a}(\psi_r))^H \boldsymbol{a}(\psi) \end{bmatrix}, \tag{6}$$

in which $\boldsymbol{a}(\psi_r)^H \boldsymbol{a}(\psi)$ produces $\boldsymbol{a}(\psi - \psi_r)$, resulting in

$$\boldsymbol{r} = \begin{bmatrix} \boldsymbol{w}_1^H \boldsymbol{a}(\psi - \psi_r) \\ \boldsymbol{w}_2^H \boldsymbol{a}(\psi - \psi_r) \end{bmatrix}. \tag{7}$$

It can be seen in the example of the Fig. 2 that the beam taper for rotation translates the *phase curve* in the graph of $\psi \times \phi$, instead of distorting it.

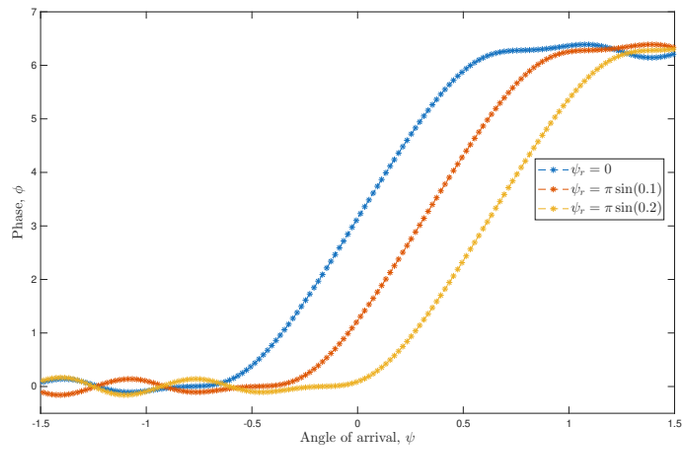

Fig. 2. Unwrapped translated *phase curve*s when applied rotation of ψ_r.

IV. Taper to phase curve linearity

When $\boldsymbol{w}_1$ and $\boldsymbol{w}_2$ are real numbers and have all elements equal, the *phase curve* is linear. This particular affirmation follows from the stronger affirmation of the following theorem.

Theorem: ϕ is linear as a function of ψ if and only if k-th element at $\boldsymbol{w}_1$ and $(k+m)$-th element at $\boldsymbol{w}_2$ are equal.

The proof is noise-free so the input signal is $\boldsymbol{x}(t) = \boldsymbol{a}(\psi)$, considering $\alpha p(t) = 1$.

From the antenna geometry, it is known that

$$\boldsymbol{w}_1^H \boldsymbol{a}(\psi) = \sum_0^{m-1} w_1^k e^{-jk\psi} \tag{8}$$

and $\boldsymbol{w}_2^H \boldsymbol{a}(\psi) = \sum_m^{2m-1} w_2^k e^{-jk\psi}$, which from (3) can be rewritten as

$$\boldsymbol{w}_2^H \boldsymbol{a}(\psi) = e^{-jm\psi} \sum_0^{m-1} w_2^{(k+m)} e^{-jk\psi}. \tag{9}$$

Comparing (8) e (9) to prove the backward affirmation, if k-th element at $\boldsymbol{w}_1$ and $(k+m)$-th element at $\boldsymbol{w}_2$ are equal, then $\boldsymbol{w}_2^H \boldsymbol{a}(\psi) = e^{-jm\psi} \boldsymbol{w}_1^H \boldsymbol{a}(\psi)$. The factor $e^{-jm\psi}$ says the *phase curve* is linear on $m\psi$, which agrees with (20).

Next it is proven the forward affirmation that linearity in *phase curve* implies that k-th element at $\boldsymbol{w}_1$ and $(k+m)$-th element at $\boldsymbol{w}_2$ are equal.

If the *phase curve* is linear then

$$\boldsymbol{w}_2^H \boldsymbol{a}(\psi) = e^{-jm\psi} \boldsymbol{w}_1^H \boldsymbol{a}(\psi).$$

Rewrite $\boldsymbol{w}_2^H \boldsymbol{a}(\psi) = e^{-jm\psi} \boldsymbol{h}_2^H \boldsymbol{a}(\psi)$ with $\boldsymbol{h}_2^k = \boldsymbol{w}_2^{(k+m)}$ for $0 \leq k \leq m-1$.

Then

$$\boldsymbol{w}_2^H \boldsymbol{a}(\psi) = e^{-jm\psi} \boldsymbol{w}_1^H \boldsymbol{a}(\psi)$$

is equivalent to

$$e^{-jm\psi} \boldsymbol{h}_2^H \boldsymbol{a}(\psi) = e^{-jm\psi} \boldsymbol{w}_1^H \boldsymbol{a}(\psi),$$

that becomes

$$\boldsymbol{h}_2^H \boldsymbol{a}(\psi) = \boldsymbol{w}_1^H \boldsymbol{a}(\psi)$$

for all ψ.

Assuming k-th elements at $\boldsymbol{w}_1$ and $\boldsymbol{h}_2$ are not all equal, then $(\boldsymbol{h}_2 - \boldsymbol{w}_1)^H \boldsymbol{a}(\psi) = \boldsymbol{0}$ is valid for all $-\pi \leq \psi \leq \pi$.

Construct m equation from m different values of ψ (in the valid interval) and obtain a complex linear system in that $(\boldsymbol{h}_2 - \boldsymbol{w}_1)$ are m variables. The complex linear system is

$$(\boldsymbol{h}_2 - \boldsymbol{w}_1)^H \boldsymbol{A} = \boldsymbol{0}, \tag{10}$$

being $\boldsymbol{A}$ a $m \times m$ matrix containing each column equal to a $\boldsymbol{a}(\psi)$ vector for a particular ψ.

The real and imaginary solutions for the real and imaginary parts of the linear system are $(\boldsymbol{h}_2 - \boldsymbol{w}_1) = \boldsymbol{0}\boldsymbol{A}^{-1} = \boldsymbol{0}$ if respective (real or imaginary) $\boldsymbol{A}$ is invertible.

This solution means all k-elements at $\boldsymbol{h}_2$ and $\boldsymbol{w}_1$ are equal, which refutes the hypothesis, implying the hypothesis is an absurd. Q.E.D.

The consequence of this theorem is that for any symmetrical bell shape beam taper, for example Hamming, Taylor, Blackmann-Harris, Nuttall, Chebyshev, is applied to beamformings, the *phase curve* becomes non linear.

V. Phase curve characterization

It is known that the phase difference, ϕ, between complex numbers t and u is the same as $t\overline{u}$. Thus, ϕ without noise due the beamformings in (4) is obtained from $\boldsymbol{w}_1^H \boldsymbol{a}(\psi)\overline{\boldsymbol{w}_2^H \boldsymbol{a}(\psi)}$, which is a trigonometric polynomial of degree $2m-1$ with real coefficients as follows.

$$y(\psi) = \sum_{0}^{m-1} w_1^k e^{-jk\psi} \left(e^{jm\psi} \sum_{0}^{m-1} w_2^{m+k} e^{jk\psi} \right) \tag{11}$$

Simplifying and rewriting with $z = e^{j\psi}$, becomes

$$y(z) = \sum_{0}^{m-1} w_1^k z^{(m-k)} \sum_{0}^{m-1} w_2^{m+k} z^k, \tag{12}$$

with ϕ the phase of $y(\psi)$.

The phase derived from the polynomial $y(z)$ characterizes exactly the *phase curve* given by any beam taper. An example of the perfect match can be seen in Fig. 3.

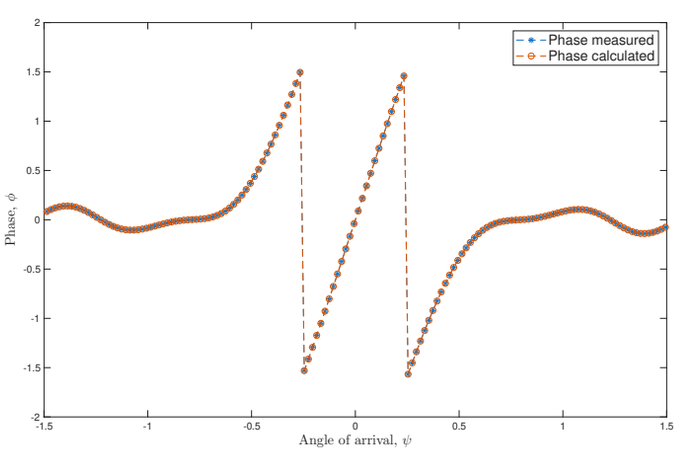

Fig. 3. Exact match between *phase curve* measured and *phase curve* evaluated from $y(z)$ in (12).

VI. ML DoA algorithm

The ML DoA algorithm which names this section is based on (12) and is going to called ML DoA.

With measured $\boldsymbol{r}$, it is necessary to find $\hat{\psi}$ that $z = e^{j\psi}$ as input to $y(z)$ produces a complex number that is most likable to be $\boldsymbol{r}$. The modification to $\boldsymbol{r}$ and the probability density function (PDF) of it is described here.

Here, the option is to estimate DoA considering the complex Gaussian ratio $\frac{r_1\overline{r_2}}{\overline{r_1}r_2}$ from the r_1 and r_2 complex Gaussian random variables because it does not depend on the signal amplitude: admit $r_1 = |r_1|e^{j\psi_1}$ and $r_2 = |r_2|e^{j\psi_2}$, then $r_1\overline{r_2} = |r_1||r_2|e^{j(\psi_1-\psi_2)}$ and $\overline{r_1}r_2 = |r_1||r_2|e^{-j(\psi_1-\psi_2)}$. The complex Gaussian ratio is

$$\frac{r_1\overline{r_2}}{\overline{r_1}r_2} = e^{2j(\psi_1-\psi_2)}, \tag{13}$$

with double the phase of interest.

A first order Taylor approximation is used to $\frac{r_1\overline{r_2}}{\overline{r_1}r_2}$ in medium and high SNR to characterize the likelihood function. To simplify expressions, r_1 and r_2 are going to be rewritten as $r_1 = a_1 + n_1$ and $r_2 = a_2 + n_2$ with $\alpha p = 1$.

First, $\overline{r_1}r_2$ can be approximate to

$$(\overline{a_1} + \overline{n_1})(a_2 + n_2) \approx \overline{a_1}a_2 + \overline{a_1}n_2 + \overline{n_1}a_2, \tag{14}$$

considering the term $\overline{n_1}n_2$ neglected.

Second, from first order Taylor approximation of $\frac{1}{1+x} \approx 1 - x$ for $x \in \mathcal{C}$ when $1 \gg x$, follows

$$\frac{1}{\overline{a_1}a_2 + \overline{a_1}n_2 + \overline{n_1}a_2} \approx \frac{1}{\overline{a_1}a_2}\left(1 - \frac{\overline{a_1}n_2 + \overline{n_1}a_2}{\overline{a_1}a_2}\right), \tag{15}$$

which is reasonably as far as $\overline{a_1}a_2 \gg \overline{a_1}n_2 + \overline{n_1}a_2$ that occurs in medium and high SNR. The ratio in (13) can be approximated to

$$\frac{r_1\overline{r_2}}{\overline{r_1}r_2} \approx \frac{a_1\overline{a_2}}{\overline{a_1}a_2} + \frac{n_1\overline{a_2} + a_1\overline{n_2}}{\overline{a_1}a_2} - \frac{a_1\overline{a_2}}{(\overline{a_1}a_2)^2}(\overline{n_1}a_2 + \overline{a_1}n_2), \tag{16}$$

which is a Gaussian distribution with the terms involving n_1 and n_2 as the white gaussian noise (WGN) with real and imaginary parts independent, and with n_1 and n_2 independent.

Expected value of $\frac{r_1\overline{r_2}}{\overline{r_1}r_2}$ is obtained from [6], [7] as follows

$$E\left[\frac{X}{Y}\right] = \frac{E[X]}{E[Y]} + \left(\frac{\rho \mathrm{STD}[X]}{\mathrm{STD}[Y]} - \frac{E[X]}{E[Y]}\right) e^{-\frac{|E[Y]|^2}{\mathrm{VAR}[Y]^2}}, \tag{17}$$

in which $E[.]$ means the expected value, VAR[.] means the variance, STD[.] means the standard deviation and ρ the correlation coefficient between X and Y.

For small VAR$[Y]$ in (17), $E\left[\frac{X}{Y}\right] \approx \frac{E[X]}{E[Y]}$, then the Probability Density Function (PDF) is

$$p(\boldsymbol{r}; z) = \left(2\pi\sigma_{WGN}^2\right)^{-1/2} e^{-\frac{\Lambda(z)}{2\sigma_{WGN}^2}}, \tag{18}$$

with the log-likelihood expression being

$$\Lambda(z) = \left(\frac{r_1\overline{r_2}}{\overline{r_1}r_2} - \frac{y(z)}{\overline{y(z)}}\right)^2. \tag{19}$$

An Expectation–Maximization Algorithm [1] for the ML estimation considers the initial value of $\hat{\psi}_0 = \frac{\hat{\phi}}{m}$ seen next in (20).

The signals from DoA θ at the ULA at an instant have inter-element phase difference

$$\phi_d = \frac{2\pi d \sin(\theta)}{\lambda}$$

without beam taper. Extending to the phase difference, ϕ, between the geometrical centers of the two beamformings it is

$$\phi = \frac{2\pi D \sin(\theta)}{\lambda} = \psi m$$

when $D = \frac{N_a d}{2} = md$ and $d = \lambda/2$. In this case, ψ is estimated by

$$\hat{\psi} = \frac{\hat{\phi}}{m}. \tag{20}$$

The steps of i-th iteration are to calculate $z = e^{j\psi}$ for all ψ around $\hat{\psi}_i$, evaluate $\Lambda(z)$ for all z with (12) and (19), and find

$$\hat{\psi}_{i+1} = \underset{\psi}{argmin}\ \{\Lambda\}. \tag{21}$$

Stop iterations when $|\hat{\psi}_{i+1} - \hat{\psi}_i| \leq \delta$, being δ a small value.

The Cramer-Rao Lower Bound (CRLB) is based on General CRLB for Signal in WGN [8] and is expressed as

$$\text{VAR}[\hat{\psi}] \geq \sigma^2_{WGN} \left(\frac{\partial \left(\frac{y}{\overline{y}}\right)}{\partial z} \frac{\partial z}{\partial \psi} \right)^{-2}, \tag{22}$$

in which

$$\frac{\partial \left(\frac{y}{\overline{y}}\right)}{\partial z} = \frac{y'\overline{y} - y\overline{y}'}{\overline{y}^2}; \tag{23}$$

and from (12)

$$y' = \sum_0^{m-1} (m-k) w_1^k z^{(m-k-1)} \sum_0^{m-1} w_2^{m+k} z^k + \sum_0^{m-1} w_1^k z^{(m-k)} \sum_0^{m-1} k w_2^{m+k} z^{k-1}; \tag{24}$$

$$\overline{y} = \sum_0^{m-1} w_1^k z^{-(m-k)} \sum_0^{m-1} w_2^{m+k} z^{-k}; \tag{25}$$

$$\overline{y}' = -\sum_0^{m-1} (m-k) w_1^k z^{-(m-k+1)} \sum_0^{m-1} w_2^{(m+k)} z^{-k} + \sum_0^{m-1} w_1^k z^{-(m-k)} \sum_0^{m-1} (-k) w_2^{(m+k)} z^{(-k-1)}; \tag{26}$$

$$\frac{\partial z}{\partial \psi} = jz; \tag{27}$$

$$\frac{\partial \overline{z}}{\partial \psi} = -j\overline{z} \tag{28}$$

for the chain rule; and σ^2_{WGN} is the variance of WGN in (16) as seen next

$$\sigma^2_{WGN} = \text{VAR}\left[\frac{n_1\overline{a_2} + a_1\overline{n_2}}{\overline{a_1}a_2} - \frac{a_1\overline{a_2}}{(\overline{a_1}a_2)^2}(\overline{n_1}a_2 + \overline{a_1}n_2) \right], \tag{29}$$

because $\frac{a_1\overline{a_2}}{\overline{a_1}a_2}$ is a constant in (16).

Considering the values that follows to calculate the variance

$$R_1 = \frac{\overline{a_2}}{\overline{a_1}a_2} - \frac{a_1\overline{a_2}}{(\overline{a_1}a_2)^2} a_2, \tag{30}$$

$$I_1 = \frac{\overline{a_2}}{\overline{a_1}a_2} + \frac{a_1\overline{a_2}}{(\overline{a_1}a_2)^2} a_2, \tag{31}$$

$$R_2 = \frac{a_1}{\overline{a_1}a_2} - \frac{a_1\overline{a_2}}{(\overline{a_1}a_2)^2} \overline{a_1}, \tag{32}$$

$$I_2 = \frac{a_1}{\overline{a_1}a_2} + \frac{a_1\overline{a_2}}{(\overline{a_1}a_2)^2} \overline{a_1}. \tag{33}$$

The variance σ^2_{WGN} is

$$\sigma^2_{WGN} = \frac{\sigma_1^2}{2}(|R_1|^2 + |I_1|^2) \sum_k |w_1^k|^2 + \frac{\sigma_2^2}{2}(|R_2|^2 + |I_2|^2) \sum_k |w_2^k|^2), \tag{34}$$

in which σ_1^2 is the variance of noise n_1, and σ_2^2 is the variance of noise n_2.

VII. Performance Evaluation

The ML DoA algorithm is evaluated with SNR 10 dB. The ULA contains $N_a = 20$ elements equispaced $d = \frac{\lambda}{2}$. Carrier frequency at 1 GHz. Monte Carlo method is using 2000 independent samples. The performance comparison is done against the classical phase monopulse and a linear interpolation of the phase monopulse ratio called "MP Interpolation", which performed good accordingly to [5].

It is seen in Fig. 4 that ML DoA and MP interpolation agrees over a large azimuth range in mean square error.

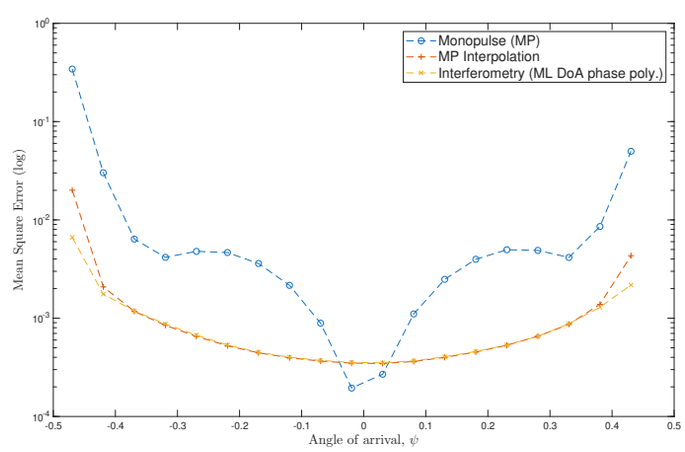

Fig. 4. Mean square error of the performance evaluation.

As expected, monopulse is biased as seen in Fig. 5 as target moves off-boresight, in azimuth, from the ULA direction while MP interpolation and ML DoA are approximately unbiased.

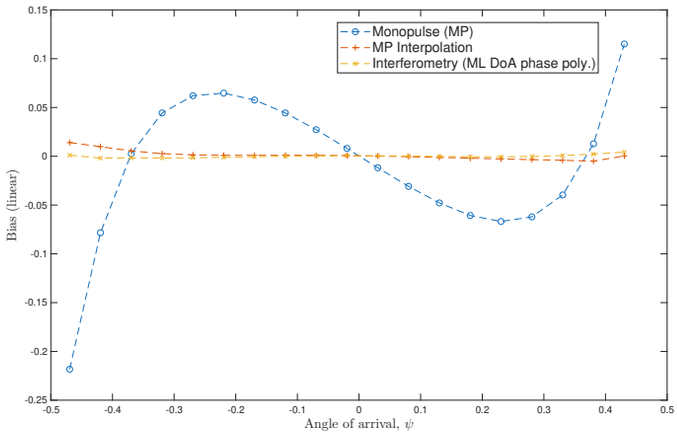

Fig. 5. Bias of the performance evaluation.

Fig. 6 shows that ML DoA and MP interpolation agrees in variance, and both are close to the CRLB from the PDF in (18). The variance of the classical monopulse performs better in target on-boresight.

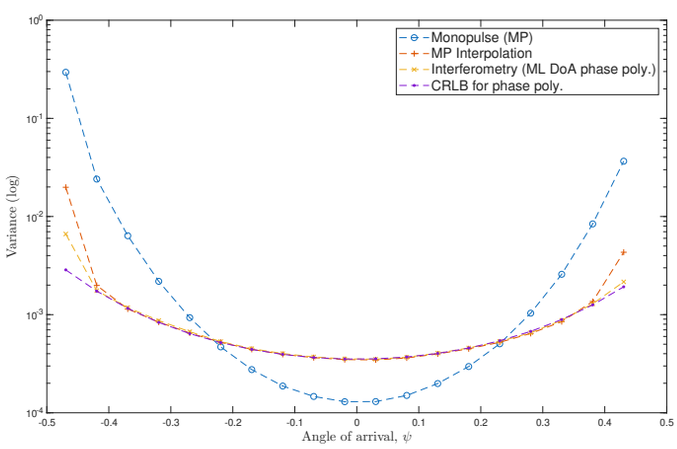

Fig. 6. Variance of the performance evaluation.

VIII. Conclusion

It is shown in the paper that a taper for rotation provokes a *phase curve* translation, instead of a distortion. This understanding allows a centralization of the *phase curve* to improve its analytical characterization. In the search for a taper to keep phase linearity, the analysis concluded that there is no such a symmetrical non-constant taper, which excluded the search for it.

The polynomial in (12) has given a clear description of the *phase curve*, which was used to a ML DoA algorithm. From the PDF that permitted the log-likelihood in (19), the CRLB was encountered to mathematically support the evaluation.

It is shown that the ML DoA estimator, based in a Taylor first order approximation, performs similar to the linear interpolation of phase monopulse [5], and the first is very close to the CRLB for the problem as well as, coincidentally, the last. The analysis makes it clear for the understanding of the unferlying trade-off between side lobes suppression and *phase curve* distortion.

This understand supports better design choices in developing an antenna array to achieve good detection and estimation coverage of the space ahead of a radar.

Referências

[1] H. Van Trees, *Detection, Estimation, and Modulation Theory, Part I: Detection, Estimation, and Linear Modulation Theory*. Wiley, 2004, no. pt. 1.

[2] D. Taggart L. Sacks, "The calculation of the phase center for spacecraft phased array antennas," in *Proceedings of MILCOM'95*, vol. 3. IEEE, 1995, pp. 1046–1050.

[3] H. Krim M. Viberg, "Two decades of array signal processing research: the parametric approach," *IEEE Signal Processing Magazine*, vol. 13, no. 4, pp. 67–94, 1996.

[4] Y.-W. Wu, S. Rhodes, E. H. Satorius, "Direction of arrival estimation via extended phase interferometry," *IEEE transactions on aerospace and electronic systems*, vol. 31, no. 1, pp. 375–381, 1995.

[5] V. A. F. S. Rita, N. S. de Farias Neto, B. C. Carvalho, I. N. F. S. Rita, "Estimação de azimute em arranjo linear de antenas com ponderações fixas (in portuguese)," in *Anais do Simpósio de Aplicações Operacionais em Áreas de Defesa (SIGE)*. São José dos Campos, Brasil: Instituto Tecnológico de Aeronáutica, 2025, p. 106–111.

[6] S. Wu, "Moments of complex gaussian ratios," *IEEE Communications Letters*, vol. 23, no. 1, pp. 88–91, 2018.

[7] Y. Li Q. He, "On the ratio of two correlated complex gaussian random variables," *IEEE Communications Letters*, vol. 23, no. 12, pp. 2172–2176, 2019.

[8] S. M. Kay, "Statistical signal processing: estimation theory," *Prentice Hall*, vol. 1, pp. Chapter–3, 1993.